AD-A059 877 NAVAL RESEARCH LAB WASHINGTON D C F/G 20/9
EMISSION OF ENERGETIC ELECTRONS FROM A ND-LASER-PRODUCED PLASMA--ETC(U)
AUG 78 C M ARMSTRONG, B H RIPIN, F C YOUNG

UNCLASSIFIED NRL-MR-3829 NL

1 OF 1
AD A059877

END
DATE FILMED
12-78
DDC

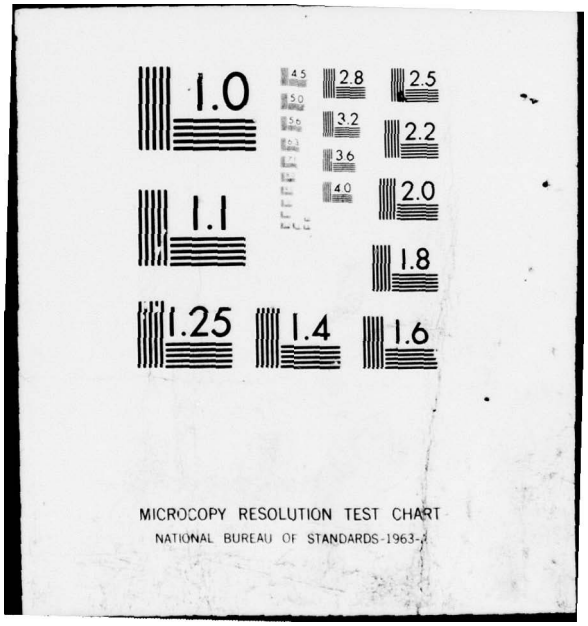
1.0
1.1
1.25
1.4
1.6
1.8
2.0
2.2
2.5
2.8
3.2
3.6
4.0
4.5
5.0
5.6
MICROCOPY RESOLUTION TEST CHART
NATIONAL BUREAU OF STANDARDS-1963-A

LEVEL II

NRL Memorandum Report 3829

Emission of Energetic Electrons from a Nd-Laser-Produced Plasma

C.M. Armstrong, B.H. Ripin, F.C. Young
R. Decoste, R.R. Whitlock, and S.E. Bodner

August 1978

Work performed at the Naval Research Laboratory under the auspices of the U.S. Department of Energy.

NAVAL RESEARCH LABORATORY
Washington, D.C.

SECURITY CLASSIFICATION OF THIS PAGE (When Data Entered)

REPORT DOCUMENTATION PAGE

READ INSTRUCTIONS BEFORE COMPLETING FORM

1. REPORT NUMBER (14) NRL-MR-
NRL Memorandum Report 3829

2. GOVT ACCESSION NO.

3. RECIPIENT'S CATALOG NUMBER

4. TITLE (and Subtitle)
(6) EMISSION OF ENERGETIC ELECTRONS FROM A Nd-LASER-PRODUCED PLASMA

5. TYPE OF REPORT & PERIOD COVERED
(9) Interim report on a continuing NRL problem.

6. PERFORMING ORG. REPORT NUMBER

7. AUTHOR(s)
(10) C.M. Armstrong*, B.H. Ripin††, F.C. Young**, R. Decoste†, R.R. Whitlock** and S.E. Bodner††

8. CONTRACT OR GRANT NUMBER(s)

9. PERFORMING ORGANIZATION NAME AND ADDRESS
Naval Research Laboratory
Washington, D.C. 20375

10. PROGRAM ELEMENT, PROJECT, TASK AREA & WORK UNIT NUMBERS
NRL Problem H02-29A

11. CONTROLLING OFFICE NAME AND ADDRESS
Department of Energy
Washington, D.C. 20545

(11) 12. REPORT DATE
August 1978

13. NUMBER OF PAGES
23

14. MONITORING AGENCY NAME & ADDRESS (if different from Controlling Office)
(12) 24 p.

15. SECURITY CLASS. (of this report)
UNCLASSIFIED

15a. DECLASSIFICATION/DOWNGRADING SCHEDULE

16. DISTRIBUTION STATEMENT (of this Report)
Approved for public release; distribution unlimited.

17. DISTRIBUTION STATEMENT (of the abstract entered in Block 20, if different from Report)

18. SUPPLEMENTARY NOTES
Work performed at the Naval Research Laboratory under the auspices of the Department of Energy.
*Supported by a National Research Council Associateship, present address: North Carolina State University, P.O. Box 5342, Raleigh, NC 27650.
(Continues)

19. KEY WORDS (Continue on reverse side if necessary and identify by block number)
Electrons
Laser-produced plasmas
about 10 to the 10th power
10 to the 15th power ≤ 10 to the 16th power
5g/cm.

20. ABSTRACT (Continue on reverse side if necessary and identify by block number)
Absolute spectral measurements of 50-500 keV electrons emitted from a Nd-laser-produced plasma are presented. For normally incident irradiation (10^{15}-10^{16} W/cm^2) onto polystyrene slab targets a total emission of $\sim 10^{10}$ electrons is inferred with a total emitted energy of $\sim$ 0.2 mJ. The electron emission is observed to be almost the same both in and out of the plane of polarization. Properties of the emitted spectrum, such as spectral hardness and intensity are observed to be dependent on pulse shape and target material.
about

DD FORM 1 JAN 73 1473 EDITION OF 1 NOV 65 IS OBSOLETE
S/N 0102-014-6601

SECURITY CLASSIFICATION OF THIS PAGE (When Data Entered)

Emission of Energetic Electrons from a Nd-Laser-Produced Plasma

I. INTRODUCTION

The absorption of laser light in laser-produced-plasmas at high irradiance ($> 10^{15}$ W/cm^2) is generally believed to be dominated by collective processes such as resonant absorption[1] and parametric instability heating.[2] Simulations typically show that the electron velocity distributions generated by these collective mechanisms exhibit long energetic tails.[3-6] The magnitude of this energetic component (electron energy > bulk plasma thermal energy) and its dominant production mechanisms are of importance to laser initiated inertial confinement fusion since the energetic electron component can result in a degradation of the energy coupling to the target through core preheat[7] and ion acceleration.[8] Previously, properties of the energetic component of the electron energy distribution have been inferred from X-ray measurements[9] and to a lesser degree from energetic ion[10] and electron[11] emissions. In this paper measurements of the energetic electron emission from a Nd-laser-produced plasma are presented for different laser pulse and target conditions.

One mechanism which can generate energetic electrons is resonance absorption. In this process the radiation is assumed obliquely incident on a varying plasma density profile. Near the laser critical density (laser frequency = plasma frequency) electron plasma waves

Note: Manuscript submitted July 11, 1978.

are excited by the longitudinal component of the radiation electric field. The subsequent damping of these large amplitude plasma waves, as they propagate toward lower density, constitutes an important plasma heating mechanism. It is noted that resonance absorption is expected even for target illuminations in which the target surface is normal to the laser beam axis. This is a consequence of the fact that, in focusing the radiation onto the target surface, some of the rays will be at oblique incidence. In addition, induced scattering,[12] filamentation,[13] and rippling of the critical surface[14] all can result in obliquely incident radiation near the critical surface.

The other main process for producing energetic electrons is instability heating. If the radiation intensity exceeds a threshold value determined by dissipation and plasma inhomogeneity considerations,[15] the laser electric field can drive parametric instabilities in which electron and ion waves exponentiate from the plasma noise level. Suprathermal electrons are then generated through the Landau damping of the high phase velocity electron plasma waves. Instability heating can occur at both critical and subcritical plasma densities. Near the critical density electron heating can occur as the result of the decay of the incident electromagnetic (EM) wave into an electron plasma wave and an ion acoustic wave (parametric decay instability).[4] The decay waves in the parametric decay instability propagate in the plane of polarization of the laser primarily along the radiation electric field. In the underdense region, near quarter-critical plasma density, instability heating can occur from the decay of the incident

EM wave into either a backscattered EM wave plus an electron plasma wave (Raman instability)[5] or two electron plasma waves (two plasmon decay instability).[6] In the Raman instability the plasma wave propagates along the direction of the incident EM wave, while in the two plasmon decay instability the plasma waves propagate at an oblique angle from the incident wave vector in the plane of polarization of the laser.

Polarization measurements of the emitted electrons should, therefore, provide information as to the dominant absorption mechanism.[16] These measurements are presented here. For normally incident irradiation (7×10^{15} W/cm^2) onto polystyrene slab targets the electron emission is observed to be approximately isotropic with respect to the polarization plane of the incident beam. This result is consistent with resonant absorption. Further information on the absorption process may also be obtained from an examination of the properties of the emitted electron energy distribution. For example, the hardness of the emitted electron energy spectrum is observed to depend on the laser pulse shape. Typically, a hardening of the spectrum is observed when moderate prepulse energy is introduced. This observation may indicate the presence of parametric instability heating in the underdense preformed plasma.

II. EXPERIMENTAL METHOD

The laser used for these experiments is one beam of the NRL Pharos II Nd-glass laser system ($\lambda_o = 1.06$ μm) delivering single 75 psec (FWHM) pulses incident onto polished planar slab targets in an

evacuated chamber ($\sim 10^{-4}$ Torr) with an irradiance between 10^{15} W/cm^2 and 10^{16} W/cm^2 through an f/1.9 aspheric lens. For all measurements reported here the laser beam axis was normal to the target surface. Absolute spectral measurements are made of electrons (50-500 keV) emitted from the plasma with two identical ($\pm$ 10%) magnetic electron spectrometers. The spectrometer design utilizes a 180° focusing permanent magnet for momentum selection with a photographic emulsion (Kodak-No-Screen) positioned at the focal plane as a passive electron detector. The compactness of the spectrometer allows it to be placed inside the target chamber at various angles from the target normal. The spectrometers possess an energy resolution ($\Delta E/E$) which spans from $\sim$ 20% at 50 keV, $\sim$ 13% at 100 keV, to $\sim$ 4% at 500 keV. The low energy cutoff of the spectrometer is determined by three factors: film sensitivity roll-off, deflection in the magnet fringe field and electron straggling in the 1000 Å aluminum overcoated 1.5 μm Kimfol entrance window. It was set at 50 keV for our instruments by comparing the shape of the beta spectrum measured for a Cs^{137} source with published spectra.[17] The sensitivity of the spectrometer in these experiments is determined by the minimum electron exposure ($\sim 2 \times 10^5$ electrons/cm^2) required to produce a recordable film exposure (0.02 density units) above fog level. For typical electron emission measurements from polystyrene targets, an instrument energy range of 50-250 keV is achieved with a dynamic range of $\sim$ 25.

To generate absolute spectra from the film exposure, the dependence of the film density on electron exposure (H-D curve) was

obtained at electron energies of 200 keV and 300 keV using a calibrated Cs^{137} beta source. The absolute sensitivity of the film at these energies was found to agree within 15% with the results of a previous calibration.[18] The discrepancy between the two absolute calibrations is presumably due to differences in film densitometry and minor changes in the film made by the manufacturer during the interval between the two calibrations. Electron energy spectra are reconstructed by using the measured absolute H-D curve obtained at 200 keV while incorporating the published[18] relative variation in film sensitivity with electron energy. The emitted electron energy distributions are then generated from the spectral measurements by correcting for the electron transmission efficiency[19] through the thin foil entrance window of the spectrometer. This correction represents the effect of the multiple scattering of the incident electrons out of the solid angle of the spectrometer. The mean square angle of multiple scattering for the 1.5 μm polycarbonate Kimfol foil used in this experiment was obtained as a function of the incident electron energy from the values calculated[20] for a 1.5 μm carbon foil. Typically, the transmission efficiency correction results in a 10% increase in the total number of electrons inferred from the spectrum.

III. SPECTRAL MEASUREMENTS

A. Electron Energy Distribution-Polystyrene Slab Target

The energy distribution (i.e., the number of electrons per unit energy interval versus the electron energy in keV) of 50-250 keV electrons detected from a planar polystyrene slab target is presented

in Fig. 1. The spectrum represents the average of eight spectra obtained in and out of the plane of polarization of the laser at observation angles of 40° and 80° from the target normal. Isotropic emission into a 2π solid angle has been assumed. From the spectrum presented in Fig. 1, a total emission of $\sim 10^{10}$ electrons is inferred with a total energy of ~ 0.2 mJ. Therefore only $\sim 3 \times 10^{-5}$ of the incident laser energy (~ 8 J) is accounted for in the emitted energetic electrons. However, as will be shown, the electron emission is not perfectly isotropic. Furthermore, the electron emission directed back toward the lens has not been measured. Therefore this assessment of the emitted electron energy will serve as a lower bound. The small fraction of the incident laser energy in energetic electrons may imply an efficient transfer of electron energy to thermal energy in the plasma or to directed ion energy.

An effective temperature, kT_e, of the electron distribution can be obtained by assuming a Maxwellian energy distribution of the form

$$f(E) = \frac{2N_o}{\pi^{\frac{1}{2}} (kT_e)^{\frac{3}{2}}} \; E^{\frac{1}{2}} \exp - (E/kT_e)$$

where E is the electron energy and N_o is the total number of electrons. From the slope of the $\ell n(f(E)/E^{\frac{1}{2}})$ vs E curve an effective temperature of $kT_e = 42 \pm 1$ keV (dashed curve Fig. 1) is obtained. This value for the hot electron temperature is in good agreement with the mean value of 50 ± 10 keV obtained from the corresponding temporally and spatially integrated X-ray bremsstrahlung spectra in the 100-300 keV photon energy region.

The mean energy, $\mathcal{E}$, of resonantly heated electrons expected in this experiment can be calculated in the cold plasma "wavebreaking"[21] limit, $\mathcal{E} = eE_dL$, where E_d is the longitudinal electric field at the resonance point and L is the density profile scale length. For a linear density profile, the evanescent electric field, E_d, can be related to the component of the free space radiation electric field in the plane of incidence, E_o, by[22]

$$E_d = \frac{E_o \phi(\tau)}{\sqrt{2\pi k_o L}} \quad .$$

The resonance function $\phi(\tau)$ is given by Ginzburg[22] with τ defined by $\tau = (k_oL)^{\frac{1}{3}} \sin\theta$, where θ is the angle of incidence. In this experiment the radiation had equal s (i.e., perpendicular to the plane of incidence) and p (i.e., parallel to the plane of incidence) polarization components. For a laser intensity of 7×10^{15} W/cm^2, scale length L = 1 μm, and angle of incidence $\theta = 15^o$ (maximum half angle of f/1.9 lens), a mean electron energy of $\mathcal{E}$ = 30 keV is obtained. This yields a resonantly heated electron temperature of 20 keV, which is approximately two times lower than the effective electron temperature inferred from the measured spectra. Some factors which could give rise to a high effective temperature are the multiple passing of the nearly collisionless high energy electrons through the heating region as they oscillate in the space charge potential well associated with the ion expansion[8] and the preferential transfer of energy from lower energy electrons to the ions. This may

indicate that quantitative features of the heated electron distribution cannot be inferred from the emitted electron spectrum without knowledge of the spatial and temporal evolution of the potential experienced by the escaping electrons.

B. Polarization Measurements of the Emitted Electrons

To determine the isotropy of the electron emission with respect to the polarization plane of the incident laser beam, electron energy spectra were recorded simultaneously in both planes using two identical (± 10%) spectrometers. Emitted electron energy spectra obtained both in and out of the plane of polarization at observation angles of 40° and 80° from the target normal are presented in Fig. 2. Electron emission is observed to decrease by 1.5 in number and by 2 in emitted energy as the observation angle is increased from 40° to 80°. As can be seen from Fig. 2 only a modest asymmetry in electron emission with respect to the laser polarization plane is observed at either angle. For example, at an observation angle of 40° the fractional increase in the total emitted electron energy in the plane of polarization ($E_{\parallel}$) over that obtained in the plane normal to it ($E_{\perp}$), is $E_{\parallel}/E_{\perp} = 1.25 \pm 0.1$, while at 80° the emitted energy anisotropy is $E_{\parallel}/E_{\perp} = 1.2 \pm 0.1$. The observed 20% anisotropy in total emitted energy is primarily the result of the anisotropy in electron emission at the higher electron energies. To insure that this asymmetry was not an artifact of the instrumentation, polarization measurements were obtained in which the spectrometers were interchanged. The measurements verify that the asymmetry remains upon interchanging the spectrometers.

The electron emission observed in this experiment is consistent with resonant absorption, which accelerates electrons along the density gradient, and with the Raman instability which heats electrons along the direction of the incident EM wave vector. The Raman instability, however, has a high intensity threshold,[23] $I > 7 \times 10^{15}$ W/cm^2 for a 10 μm scale length, and, therefore, is not expected in this experiment. The electron emission is, moreover, inconsistent with significant heating from both the parametric decay and two plasmon decay instabilities which preferentially heat electrons in the plane of polarization. However, scattering from the space charge potential,[8] rippling of the critical surface,[14] and strong magnetic fields[24] all could tend to isotropize the heated electron distribution. When viewed in this light the asymmetry in electron emission noticed at the higher electron energies could represent the signature of parametrically heated electrons, which due to their high energy are relatively unaffected by the various isotropizing mechanisms.[25]

C. Electron Energy Distribution-Preformed Plasma

To simulate the effect of a temporally shaped laser pulse on the electron emission, spectral measurements were obtained in experiments in which a prepulse-formed plasma is irradiated with the short, high-irradiance main pulse.[26] The relative timing of the prepulse to the main pulse was set at 2 nsec while the relative amplitudes were adjusted by varying the attenuation ratio. The low density, long scale length ($\sim$ 100 μm) prepulse-formed plasma is expected to lower the threshold for the excitation of parametric instabilities in the underdense plasma. A single electron spectrometer viewed the

target at an angle of 45° from the normal, midway between the laser polarization planes, in this series of measurements. A decrease in electron emission is typically observed as the prepulse level is increased. This is believed to be a result of the reduced absorption resulting from a backscatter instability.[26] However, for moderate prepulse strengths ($\sim$ 10% of the incident energy) electron energy distributions are observed (Fig. 3) which exhibit an enhanced hard component (above 140 keV) over typical spectra obtained without a prepulse. From the distribution (solid curve) in Fig. 3, a total emission of 4×10^{10} electrons is inferred with an energy of 1.0 mJ. This represents an increase of ~ 4 over electron emission typically obtained without a prepulse. Note that the total emitted energy obtained with the prepulse still represents only $\sim 10^{-4}$ of the incident energy. Electron spectra obtained when the preformed plasma is present are observed to be non-Maxwellian, as shown in Fig. 3. For example, the emitted electron energy spectrum (i.e., the emitted energy per unit energy interval versus the electron energy in keV), shown in Fig. 3 (dashed curve), indicates that 40% of the total emitted energy resides within 210 $\pm$ 30 keV. Such highly non-Maxwellian energy distributions may imply an enhanced level of parametric instability heating in the underdense region, although emission polarization measurements would be useful to strengthen this inference.

D. Electron Energy Distribution - Aℓ Slab Target

Measurements of electron emission from aluminum targets were also obtained (Fig. 4) which suggest a dependence on target material. Spectral measurements from Aℓ slab targets, obtained without an

applied prepulse, at an angle of 45° from the target normal, midway between the laser polarization planes, indicate over an order of magnitude increase in electron emission (5×10^{11} electrons) and emitted energy (13.6 mJ) over that observed at similar irradiance levels from plastic targets.[27] This increase in emission may reflect an increase in heating resulting from electron reflection off the ($Z = 13$) overdense plasma into the heating region and/or a reduction in the charge separation electric field due to the presence of the grounded conducting target.

IV. CONCLUSIONS AND SUMMARY

In summary, spectral measurements of energetic electrons emitted from a Nd-laser-produced plasma account for only a small fraction ($\sim 10^{-4}$) of the incident laser energy. This implies a low level production and/or a loss of energy through ion acceleration. For normally incident irradiation, the electron emission from polystyrene slab targets is observed to be approximately isotropic with respect to the polarization plane of the incident beam. This result is consistent with resonant absorption. On the other hand, energy distributions obtained when moderate prepulse energy is introduced typically exhibit an enhanced high energy component, implying the possibility of parametric heating in the underdense plasma. It is noted, however, that measurement of the target potential and modeling of the effect of the space charge electric field on the emitted electron energy distribution are required before specific comparisons between the

emitted electron energy distribution and the heated electron distribution can be made.

ACKNOWLEDGMENT

It is a pleasure to acknowledge the laser expertise of J. M. McMahon which made these experiments possible.

REFERENCES

1. J. P. Freidberg, R. W. Mitchell, R. L. Morse, and L. F. Rudsinski, Phys. Rev. Lett. 28, 795 (1972).
2. D. F. Dubois and M. V. Goldman, Phys. Rev. 164, 207 (1967); K. Nishikawa, J. Phys. Soc. Jap. 24, 916, 1152 (1968); P. K. Kaw and J. Dawson, Phys. Fluids 12, 2586 (1969).
3. K. Estabrook and W. L. Kruer, Phys. Rev. Lett. 40, 42 (1978); C. P. DeNeef and J. S. DeGroot, Phys. Fluids 20, 1074 (1977); K. G. Estabrook, E. J. Valeo, and W. L. Kruer, Phys. Fluids 18, 1151 (1975).
4. J. S. DeGroot and J. I. Katz, Phys. Fluids 16, 401 (1973); W. L. Kruer and J. M. Dawson, Phys. Fluids 14, 1003 (1971); J. J. Thomson, R. J. Faehl, W. L. Kruer, and S. Bodner, Phys. Fluids 17, 973 (1974).
5. W. L. Kruer, K. G. Estabrook, and K. H. Sinz, Nuc. Fusion 13, 952 (1973).
6. W. L. Kruer and J. M. Dawson, Phys. Fluids 15, 446 (1972).
7. J. L. Nuckolls, L. Wood, A. Thiessen, and G. Zimmerman, Nature (London) 239, 139 (1972).

8. R. L. Morse and C. W. Nielson, Phys. Fluids 16, 909 (1973); E. J. Valeo and I. B. Bernstein, Phys. Fluids 19, 1348 (1976).

9. J. F. Kephart, R. P. Godwin, and G. H. McCall, Appl. Phys. Lett. 25, 108 (1974); B. H. Ripin, P. G. Burkhalter, F. C. Young, J. M. McMahon, D. G. Colombant, S. E. Bodner, R. R. Whitlock, D. J. Nagel, D. J. Johnson, N. K. Winsor, C. M. Dozier, R. D. Bleach, J. A. Stamper, and E. A. McLean, Phys. Rev. Lett. 34, 1313 (1975); B. Yaakobi, I. Pelah, and J. Hoose, Phys. Rev. Lett. 37, 836 (1976).

10. R. Decoste and B. H. Ripin, Phys. Rev. Lett. 40, 34 (1978); P. M. Campbell, R. R. Johnson, F. J. Mayer, L. V. Powers, and D. C. Slater, Phys. Rev. Lett. 39, 274 (1977).

11. D. V. Giovanielli, J. F. Kephart, and A. W. Williams, J. Appl. Phys. 47, 2907 (1976); R. A. Hass, W. C. Mead, W. L. Kruer, D. W. Phillion, H. N. Kornblum, J. D. Lindl, D. MacQuiqq, V. C. Rupert, and K. G. Tirsell, Phys. Fluids 20, 322 (1977); C. M. Armstrong, R. Decoste, F. C. Young, and B. H. Ripin, Bull. Am. Phys. Soc. 22, 1128 (1977); J. L. Bocher, J. Martineau, and M. Rabeau, Bull. Am. Phys. Soc. 22, 1128 (1977); K. G. Tirsell, H. C. Catron, S. S. Glaros, H. N. Kornblum, and V. W. Slivinsky, Bull. Am. Phys. Soc. 22, 1195 (1977).

12. C. S. Liu, M. N. Rosenbluth, and R. B. White, Phys. Fluids 17, 1211 (1974).

13. A. G. Litvak, Zh. Eksp. Teor. Fiz. 57, 629 (1968) [Sov. Phys. JETP 30, 344 (1970)]; P. Kaw, G. Schmidt, and T. Wilcox, Phys. Fluids 16, 1522 (1973).

14. B. H. Ripin, NRL Memo Report No. 3591, p. 128 (1977); J. J. Thomson, W. L. Kruer, A. B. Langdon, C. E. Max, and W. C. Mead, UCRL-79628 Rev. 1 (1977).

15. F. W. Perkins and J. Flick, Phys. Fluids 14, 2012 (1971).

16. P. Kolodner and E. Yablonovitch, Phys. Rev. Lett. 37, 1754 (1976).

17. H. M. Agnew, Phys. Rev. 77, 655 (1950).

18. R. A. Dudley, Nucleonics 12, 24 (1954).

19. C. H. Chang, C. S. Cook, and H. Primakoff, Phys. Rev. 90, 544 (1953).

20. J. D. Jackson, Classical Electrodynamics, 2nd ed. (John Wiley and Sons, Inc., New York, 1975), p. 674.

21. P. Koch and J. Albritton, Phys. Rev. Lett. 32, 1420 (1974).

22. V. L. Ginzburg, The Properties of Electromagnetic Waves in Plasmas, (Pergamon, New York, 1964), p. 260.

23. C. S. Liu, in Advances in Plasma Physics, Vol. 6, edited by A. Simon and W. B. Thomson (John Wiley and Sons, Inc., New York, 1976), p. 176.

24. J. A. Stamper and B. H. Ripin, Phys. Rev. Lett. 34, 138 (1975); J. A. Stamper, E. A. McLean, and B. H. Ripin, Phys. Rev. Lett. 40, 1177 (1978).

25. B. F. Lasinski, private communication.

26. B. H. Ripin, F. C. Young, J. A. Stamper, C. M. Armstrong, R. Decoste, E. A. McLean, and S. E. Bodner, Phys. Rev. Lett. 39, 611 (1977).

27. For these measurements a somewhat thicker (6 μm) Kimfol entrance foil was used than for previous measurements.

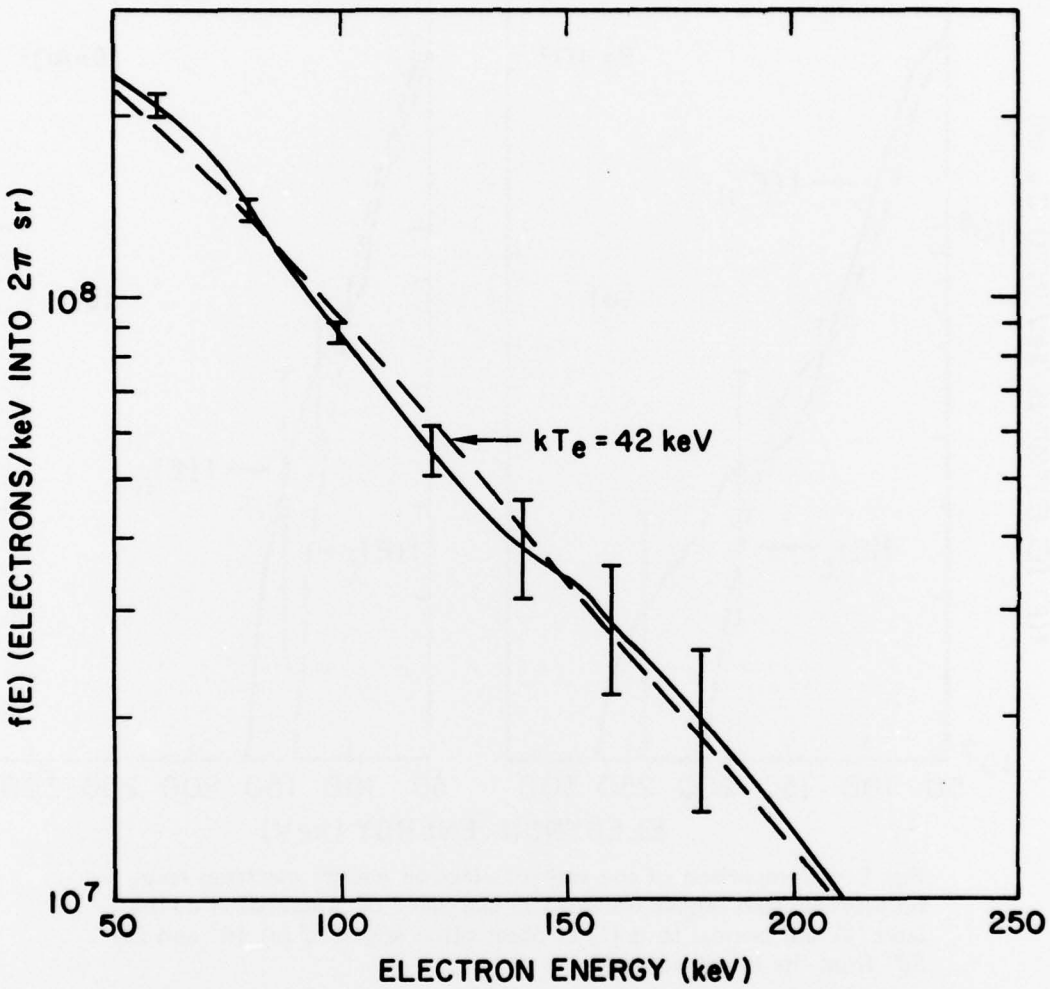

Fig. 1 — Time integrated energetic electron emission spectrum for polystyrene slab targets. The spectrum (solid curve) is the average of several spectra obtained at an average irradiance of 7×10^{15} W/cm^2, both in and out of the plane of polarization of the laser, at observation angles of 40° and 80° from the target normal. Error bars denote the standard deviation associated with the average. The dashed curve, shown in the figure, is a Maxwellian energy distribution with a temperature of kT_e = 42 keV.

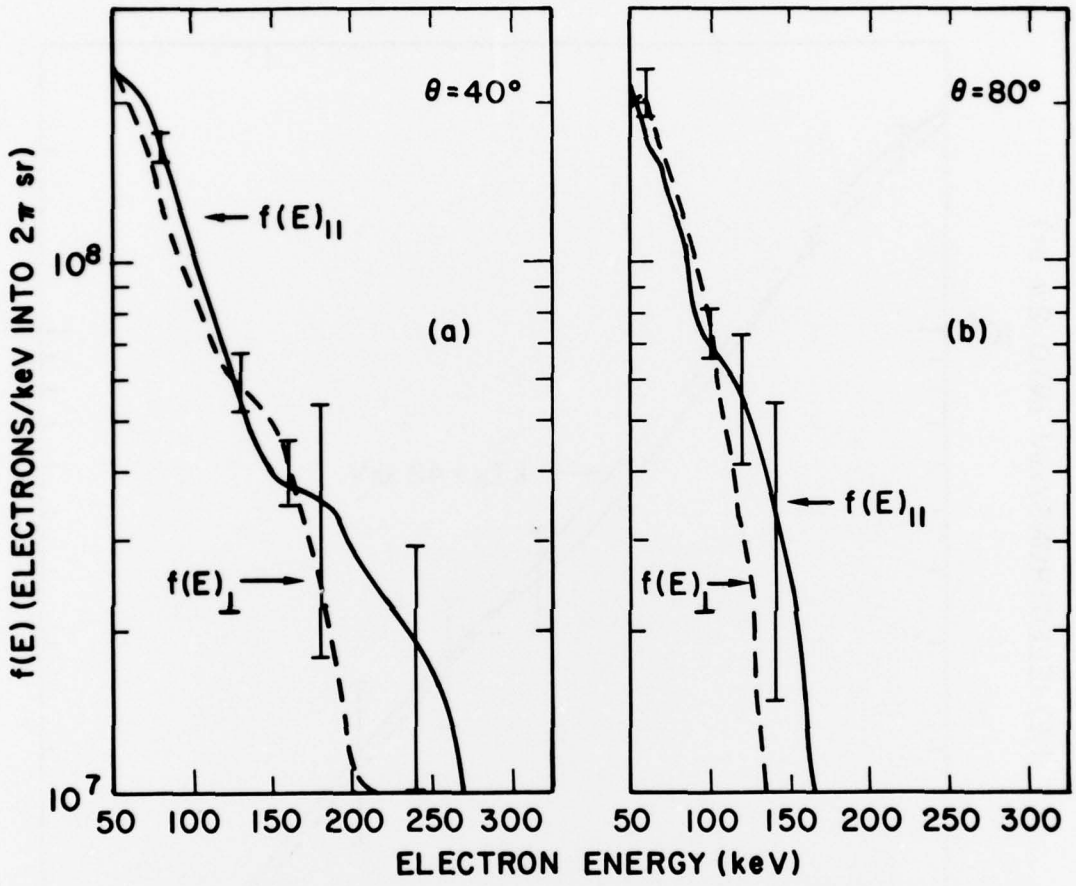

Fig. 2 — Comparison of the emitted electron energy spectrum from polystyrene slab targets obtained in the plane of polarization of the laser ($\parallel$) and normal to it ($\perp$) at observation angles of (a) 40° and (b) 80° from the target normal.

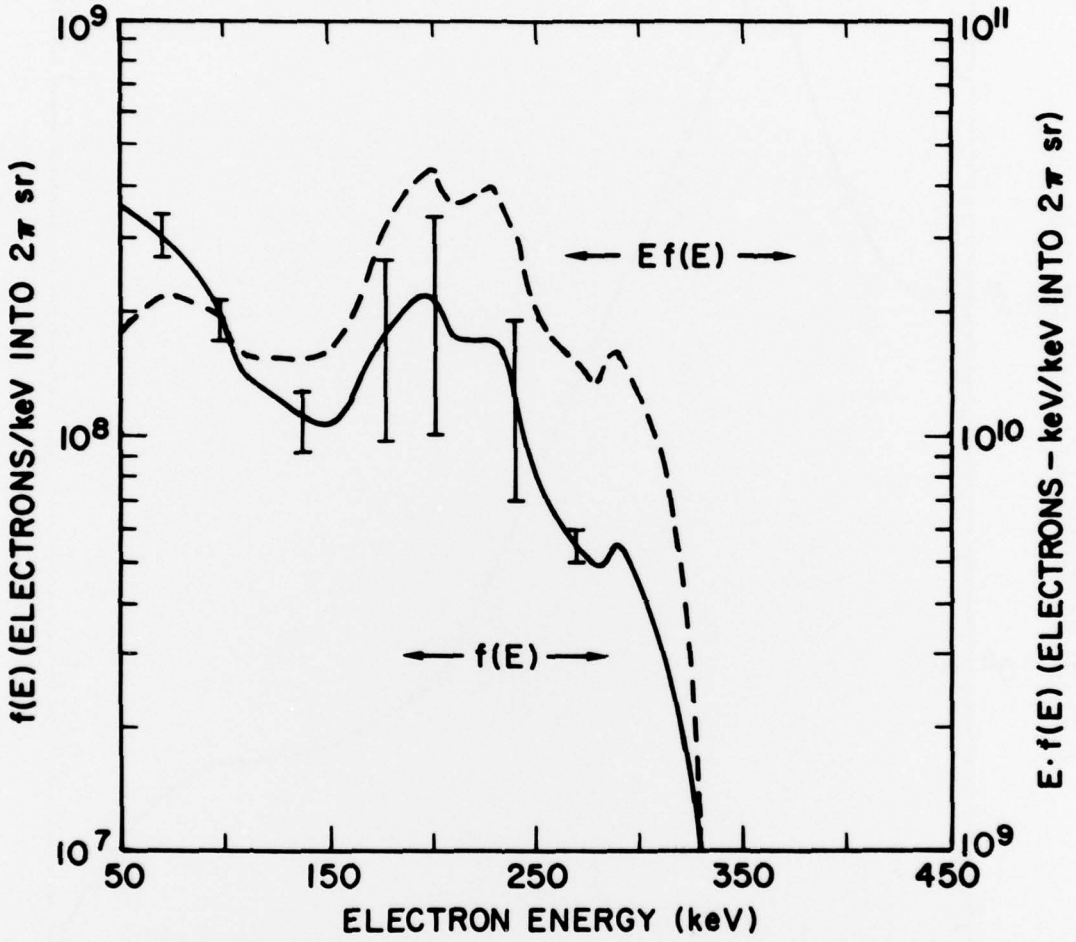

Fig. 3 — Emitted electron spectrum (solid curve) and emitted energy distribution (dashed curve) for polystyrene prepulse-formed plasmas irradiated by a high intensity ($\sim 7 \times 10^{15}$ W/cm^2) laser pulse. For the results shown here the temporal separation between the prepulse and main pulse is 2 nsec with prepulse energy/total incident energy = 0.1.

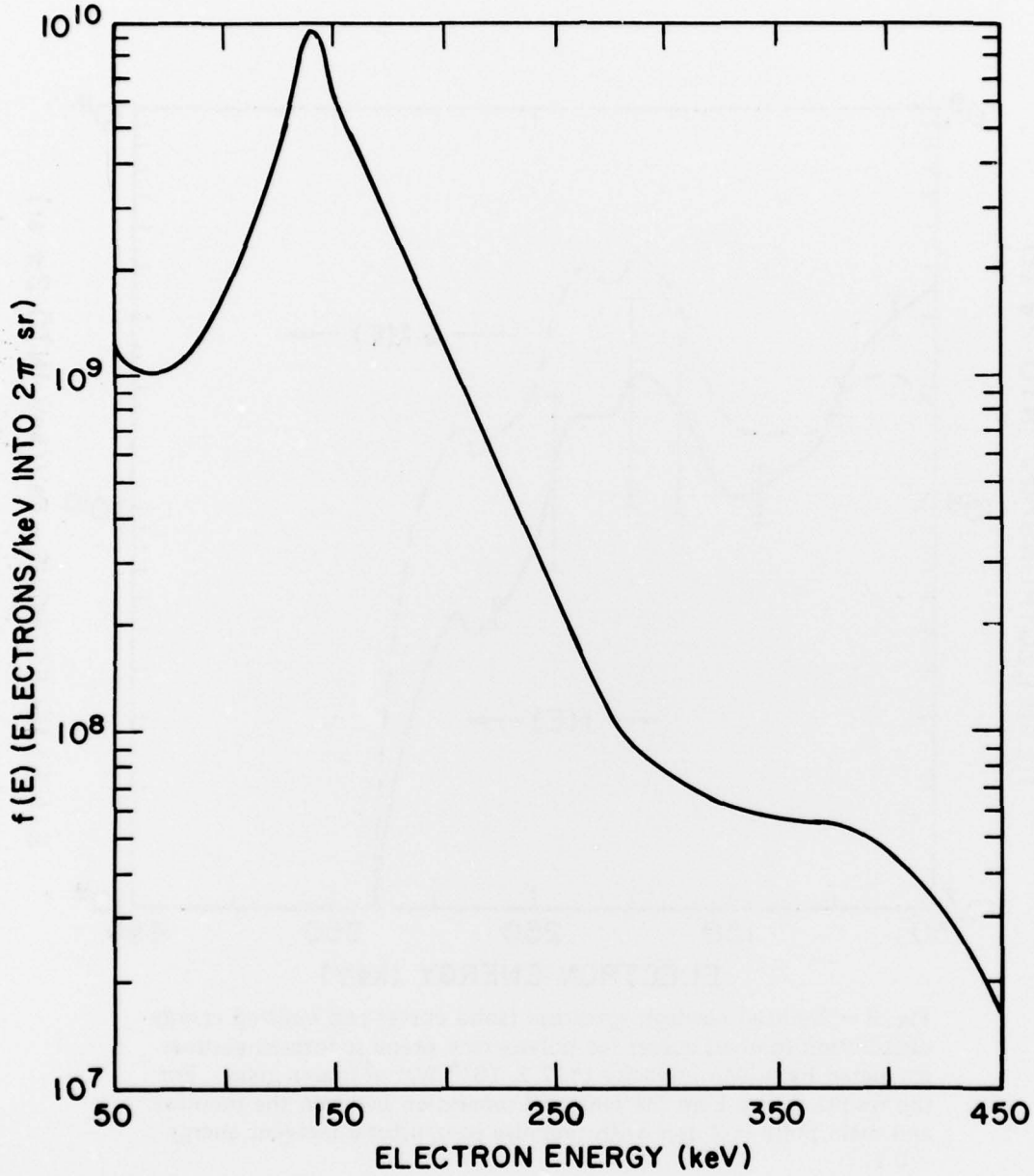

Fig. 4 — Typical emitted electron spectrum for an aluminum slab target obtained at an average irradiance of 7×10^{15} W/cm^2.